

Research Article

Effect of Viscous Dissipation on MHD Free Convection Flow Heat and Mass Transfer of Non-Newtonian Fluids along a Continuously Moving Stretching Sheet

K.C. Saha, M.A. Samad and M.R. Hossain

Department of Mathematics, University of Dhaka, Dhaka-1000, Bangladesh

Abstract: The effects of MHD free convection heat and mass transfer of power-law Non-Newtonian fluids along a stretching sheet with viscous dissipation has been analyzed. This has been done under the simultaneous action of suction, thermal radiation and uniform transverse magnetic field. The stretching sheet is assumed to continuously moving with a power-law velocity and maintaining a uniform surface heat-flux. The governing non-linear partial differential equations are transformed into non-linear ordinary differential equations, using appropriate similarity transformations and the resulting problem is solved numerically using Nachtsheim-Swigert shooting iteration technique along with sixth order Runge-Kutta integration scheme. A parametric study of the parameters arising in the problem such as the Eckert number due to viscous dissipation, radiation number, buoyancy parameter, Schmidt number, Prandtl number etc are studied and the obtained results are shown graphically and the physical aspects of the problem are discussed.

Keywords: Free convection, MHD, power-law fluid, radiation, surface heat flux, viscous dissipation

INTRODUCTION

Considerable interest has recently been shown in radiation interaction with free convection for heat transfer in fluid. This is due to the significant role of thermal radiation in the surface heat transfer when convection heat transfer is small particularly in free convection problems involving absorbing-emitting fluids. Hot rolling, drawings of plastic films and artificial fibers, glass fiber production, metal extrusion are examples of such physical applications. Many manufacturing processes involve the cooling of continuous sheets or filaments by drawing them through a quiescent fluid which are stretched during the drawing process. The final product of required characteristics depend to a great extent on the rate of cooling which can be controlled by drawing such sheets in an electrically conducting fluid and subject to magnetic field. Sakiadis (1961), first presented boundary layer flow over a continuous solid surface moving with constant speed. Elbashbeshy (1998) investigated heat transfer over a stretching surface with variable and uniform surface heat flux subject to injection and suction. Vajravelu and Hadjinicolaou (1997) studied the convective heat transfer in an electrically conducting fluid near an isothermal stretching sheet and studied the effect of internal heat generation or absorption. Also, Glauert (1961) analyzed magneto-hydro-dynamic boundary layer on a flat plate.

The study of non-Newtonian fluid flow and heat transfer over a stretched surface gets attention because numerous industrially important fluids exhibit non linear relationship between shear stress and rate of strain such as polymer solution, molten plastics, pulps, paints and foods. Rajgopal *et al.* (1984) studied flow of viscoelastic fluid over stretching sheet. Dandapat and Gupta (2005) extended the problem to study heat transfer and Datti *et al.* (2005) analyzed the problem over a non-isothermal stretching sheet. The MHD boundary layer flow over a continuously moving plate for a micropolar fluid has been studied by Rahaman and Sattar (2006) and Raptis (1998). Several authors (Anderson *et al.*, 1992; Mahmood and Mahmoud, 2006; Chen and Chen, 1988) adopted the non-linearity relation as power-law dependency of shear stress on rate of strain. Recently, Chen (2008) studied the effect of magnetic field and suction/injection on the flow of power-law non-Newtonian fluid over a power-law stretched sheet subject to a surface heat flux. All the above investigations are restricted to MHD flow and heat transfer problems. However, of late, the radiation effect on MHD flow and heat transfer problems has become more important industrially. Many processes in engineering areas occur at high temperatures and the knowledge of radiative heat transfer becomes very important for the design of the pertinent equipments. Nuclear power plants, gas turbines and the various propulsion devices for aircrafts, missiles, satellites and space vehicles are examples of such engineering areas. There are various kinds of high temperature systems

Corresponding Author: K.C. Saha, Department of Mathematics, University of Dhaka, Dhaka-1000, Bangladesh

This work is licensed under a Creative Commons Attribution 4.0 International License (URL: <http://creativecommons.org/licenses/by/4.0/>).

such as a heat exchanger and an internal combustor, in which the radiation may not be negligible in comparison with the conductive and convective heat transfer. During combustion of a hydrocarbon fuel and the particles such as soot and coal suspended in a hot gas flow absorb, emit and scatter the radiation. The interaction of radiation with hydromagnetic flow has become industrially more prominent in the processes wherever high temperatures occur. El-Hakiem (2008) investigated radiation effect on a heated surface Takhar *et al.* (1996). Analyzed the radiation effects on MHD free convection flow past a semi-infinite vertical plate using Runge-Kutta Merson quadrature. Ali *et al.* (1984) studied radiation effects on free convection flow over a horizontal plate. Chamkha *et al.* (2001) analyzed radiation effects on free convection flow past a semi-infinite vertical plate.

In the present paper, the problem studied by Chen (2008) has been extended for the case of free convection to analyze the effect of viscous dissipation. This study has also been carried out to investigate the effects of MHD free convection on both heat and mass transfer of power-law non-Newtonian fluids along a continuously moving stretching sheet.

METHODOLOGY

Governing equations: Let us consider a steady two dimensional MHD free convection laminar boundary layer flow of a viscous incompressible and electrically conducting fluid obeying the power-law model along a permeable stretching sheet under the influence of thermal radiation. Introducing the Cartesian co-ordinate system, the X-axis is taken along the stretching sheet in the vertically upward direction and the Y-axis is taken normal to the sheet. Two equal and opposite forces are introduced along the X-axis, so that the sheet is stretched. This continuous sheet is assumed to move with a velocity according to a power-law from, i.e., $u_w = Cx^p$ and be subject to a surface heat. The ambient temperature of the flow is T_∞ and the concentration of the uniform flow is C_∞ . The fluid is considered to be gray, absorbing- emitting radiation but non-scattering medium and the Rossland approximation is used to describe the radiative heat flux in the energy equation. The concentration is assumed to be non-reactive. The radioactive heat flux in the X-direction is considered negligible in comparison to the Y-direction. A strong magnetic field is comparison in comparison to the applied magnetic field. The electrical current flowing in the fluid gives rise to an induced magnetic field if the fluid was an electrical insulator, but here we have taken the fluid to be the electrically conducting. Hence, only the applied magnetic field B plays a role which gives rise to magnetic forces $F_x = \frac{\sigma B u}{\rho}$ in the X-direction, where σ is the electrical conductivity, B is the magnetic

field strength (magnetic induction) and ρ is the density of the fluid. Under the above assumptions, the governing equations for the flow fields are represented as follows:

$$\frac{\partial u}{\partial x} + \frac{\partial v}{\partial y} = 0 \tag{1}$$

$$u \frac{\partial u}{\partial x} + v \frac{\partial u}{\partial y} = \frac{K}{\rho} \frac{\partial}{\partial y} \left(\left| \frac{\partial u}{\partial y} \right|^{n-1} \frac{\partial u}{\partial y} \right) + g\beta(T - T_\infty) - \frac{\sigma B^2 u}{\rho} \tag{2}$$

$$u \frac{\partial T}{\partial x} + v \frac{\partial T}{\partial y} = \alpha \frac{\partial^2 T}{\partial y^2} - \frac{1}{\rho c_p} \frac{\partial q_r}{\partial y} + \frac{K}{\rho c_p} \left(\left| \frac{\partial u}{\partial y} \right|^{n-1} \frac{\partial u}{\partial y} \right)^2 \tag{3}$$

$$u \frac{\partial C}{\partial x} + v \frac{\partial C}{\partial y} = D_m \frac{\partial^2 C}{\partial y^2} \tag{4}$$

The radiative heat flux q_r is described by the Rosseland approximation such that:

$$q_r = - \frac{4\sigma_1}{3k_1} \frac{\partial T^4}{\partial y} \tag{5}$$

where, σ_1 is the Stefan-Boltzman constant and k_1 is the Rosseland mean absorption coefficient. It is assumed that the temperature difference within the flow is sufficiently small such that T^4 can be expressed in a Taylor series about the free stream temperature T_∞ and then neglecting higher-order terms. This results in the following approximation:

$$T^4 \approx 4T_\infty^3 T - 3T_\infty^4 \tag{6}$$

Using (5) and (6) in the last term of Eq. (3), we obtain:

$$\frac{\partial q_r}{\partial y} = - \frac{16\sigma_1 T_\infty^3}{3k_1} \frac{\partial^2 T}{\partial y^2} \tag{7}$$

Introducing q_r in Eq. (3), we obtain the following governing boundary layer equations as:

$$\frac{\partial u}{\partial x} + \frac{\partial v}{\partial y} = 0$$

$$u \frac{\partial u}{\partial x} + v \frac{\partial u}{\partial y} = \frac{K}{\rho} \frac{\partial}{\partial y} \left(\left| \frac{\partial u}{\partial y} \right|^{n-1} \frac{\partial u}{\partial y} \right) + \tag{8}$$

$$g\beta(T - T_\infty) - \frac{\sigma B^2 u}{\rho} \tag{9}$$

$$u \frac{\partial T}{\partial x} + v \frac{\partial T}{\partial y} = \alpha \frac{\partial^2 T}{\partial y^2} + \frac{16\sigma_1 T_\infty^3}{3\rho c_p k_1} \frac{\partial^2 T}{\partial y^2} + \frac{K}{\rho c_p} \left(\left| \frac{\partial u}{\partial y} \right|^{n-1} \frac{\partial u}{\partial y} \right)^2 \tag{10}$$

$$u \frac{\partial C}{\partial x} + v \frac{\partial C}{\partial y} = D_m \frac{\partial^2 C}{\partial y^2} \tag{11}$$

The appropriate boundary conditions are:

$$\left. \begin{aligned} u_w = Cx^p, v = v_w, \partial T / \partial y = -q_w / \kappa, C = C_\infty + bx \text{ at } y=0, x > 0 \\ u_w \rightarrow 0, T \rightarrow T_\infty, C \rightarrow C_\infty \text{ as } y \rightarrow \infty \end{aligned} \right\} \quad (12)$$

where, u and v are the velocity components, K is the consistency coefficient, c_p is the specific heat at constant pressure, $B(x)$ is the magnetic field, T is the temperature of the fluid layer, g is the acceleration due to gravity, β is the volumetric coefficient of thermal expansion, σ is the electric conductivity, ρ is the density of the fluid, α is the thermal diffusivity, k is the thermal conductivity of the fluid, n is the flow behavior index, q_r is the radiative heat flux. v_w is the velocity component at the wall having positive value to indicate suction and negative value for injection and q_w is surface heat flux. The power index p indicates surface is accelerated or decelerated for positive and negative values, respectively.

Similarity analysis: In order to obtain a similarity solution of the problem, we introduce a similarity parameter $\delta(x)$ such that $\delta(x)$ is a length scale. We now introduce the following dimensionless variables:

$$\eta = \frac{y}{\delta(x)} = \left(\frac{C^{2-n}}{K/\rho} \right)^{1/(n+1)} x^{\{p(2-n)-1\}/(n+1)} y \quad (13)$$

$$\psi = \left(\frac{C^{1-2n}}{K/\rho} \right)^{-1/(n+1)} x^{\{p(2n-1)+1\}/(n+1)} f(\eta) \quad (14)$$

$$\theta(\eta) = \frac{(T-T_\infty)Re_x^{1/(n+1)}}{q_w x / \kappa} \quad (15)$$

$$\phi(\eta) = \frac{C-C_\infty}{bx} \quad (16)$$

where, ψ is the stream function, η is the dimensionless distance normal to the sheet, f is the dimensionless stream function and θ and ϕ are the dimensionless fluid temperature and concentration respectively. Using the transformations from Eq. (13) to (16) in Eq. (9) to (11), we obtain the following dimensionless equations as:

$$\left(|f''|^{n-1} f'' \right)' + \frac{p(2n-1)+1}{(n+1)} f f'' - p(f')^2 - M f' + \lambda \theta = 0 \quad (17)$$

$$\frac{3N+4}{3NPr} \theta'' + \frac{p(2n-1)+1}{(n+1)} f \theta' + \frac{p(2-n)-1}{(n+1)} f' \theta + Ec(|f''|^{n-1} f'')^2 = 0 \quad (18)$$

$$\frac{1}{Sc} \phi'' + \frac{p(2n-1)+1}{(n+1)} f \phi' - f' \phi = 0 \quad (19)$$

The transformed boundary conditions are:

$$\left. \begin{aligned} f'=1, f=\frac{n+1}{p(2n-1)+1} f_w, \theta'=-1, \phi=1 \text{ at } \eta=0 \\ f' \rightarrow 0, \theta \rightarrow 0, \phi \rightarrow 0 \text{ as } \eta \rightarrow \infty \end{aligned} \right\} \quad (20)$$

where, $M = \frac{\sigma B^2 x}{\rho u_w}$ is the magnetic field parameter, $Pr = \frac{x u_w}{\alpha} Re_x^{-2/(n+1)}$ is the generalized Prandtl number, $Ec = \frac{(u_w^{n+1/2})^2}{c_p \frac{q_w}{k} x^n} Re_x^{\frac{n}{n+1}}$ is the local Eckert number due to viscous dissipation, $N = \frac{kk_1}{4\sigma_1 T_\infty^3}$ is the radiation number, $f_w = -\frac{v_w}{u_w} Re_x^{1/(n+1)}$ is the suction parameter, $\lambda = \frac{Gr}{Re_x^{1/(n+1)}} = \frac{g\beta(q_w/k)x^2}{u_w^2} Re_x^{\frac{-1}{(n+1)}}$ is the buoyancy parameter, $Sc = \frac{u_w x}{D_m} Re_x^{\frac{-2}{(n+1)}}$ is the local Schmidt number and $Re_x = \frac{\rho u_w^{2-n} x^n}{K}$ is the local Reynolds number.

Here, we note that the magnetic field strength B should be proportional to x to the power of $(p-1)/2$ to eliminate the dependence of M on x , i.e., $B(x) = B_0 x^{(p-1)/2}$, where B_0 is a constant. The parameters of engineering interest for the present problem are skin friction Coefficient (C_f), local Nusselt number (Nu_x) and local Sherwood number (Sh_x), which indicate physically wall shear stress, local wall heat transfer rate and local mass transfer rate respectively. The skin friction Coefficient (C_f) is given by:

$$C_f = \frac{\tau_w}{\frac{1}{2} \rho u_w^2} \quad \text{or, } Re_x^{1/(n+1)} C_f = 2 |f''(0)|^{n-1} f''(0) \quad (21)$$

The local Nusselt number Nu_x is defined as:

$$Nu_x = \frac{hx}{k} = \frac{Re_x^{1/(n+1)}}{\theta(0)} \quad \text{or, } Nu_x Re_x^{-1/(n+1)} = 1/\theta(0) \quad (22)$$

And the local Sherwood number (Sh) is given by:

$$Sh = \frac{xM_w}{D_m(C-C_\infty)} \quad \text{or, } Sh Re_x^{-1/(n+1)} = -\phi'(0) \quad (23)$$

Thus from Eq. (21) to (23), we see that the skin friction coefficient (C_f) local Nusselt number (Nu_x) and Sherwood number (Sh) are proportional to $2|f''(0)|^{n-1} f''(0)$, $1/\theta(0)$ and $-\phi'(0)$, respectively.

RESULTS AND DISCUSSION

The system of transformed governing Eq. (17)-(19) is solved numerically using Nachtsheim and Swigert

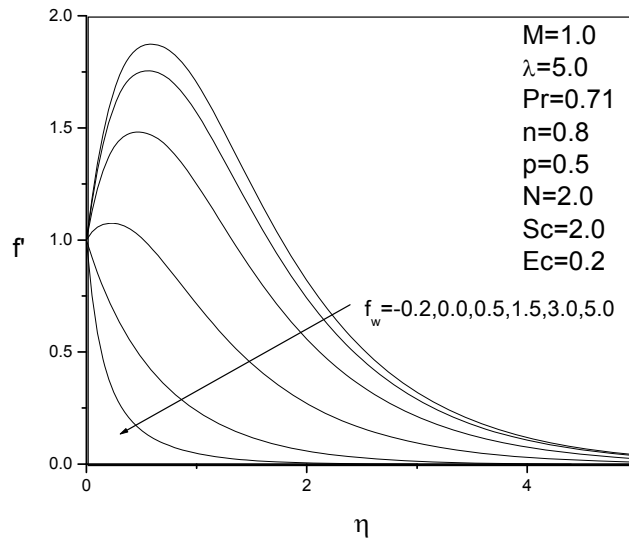


Fig. 1: Velocity profiles for different values of suction parameter (f_w)

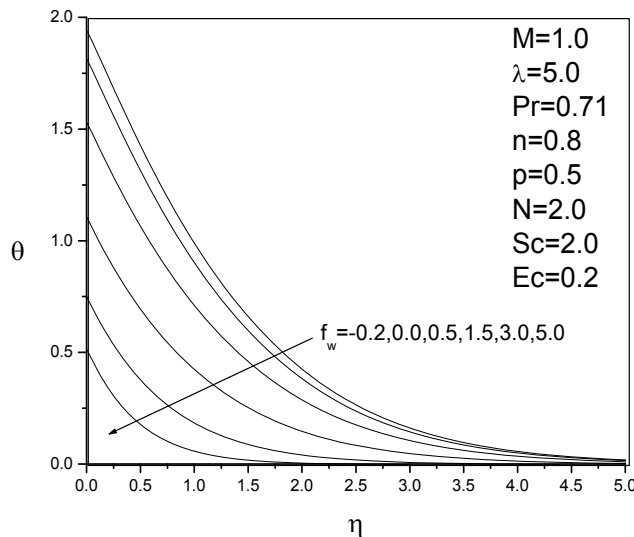


Fig. 2: Temperature profiles for different values of suction parameter (f_w)

(1965) shooting iterative technique along with sixth order Runge-Kutta integration scheme. Now in order to discuss the results, we solve the system (17)-(19) for different physically important parameters and carry out the discussion how these parameters do effect on the velocity, temperature and concentration of the flow field. The effects of suction on the velocity, temperature and concentration profiles are shown in the Fig. 1 to 3, respectively. Due to the effect of suction some of the retarded fluid particles are taken out from the boundary layer and thus prevent the boundary layer separation. We observe that the velocity profiles decrease with the increase of suction parameter. This indicates the fact that for a flow field of higher suction, the velocity of the fluid particle is low and velocity stabilizes very quickly (Fig. 1) near the stretching sheet. The negative

values of f_w indicates injection. For $f_w = -0.2$, the velocity increases at first due to buoyancy effect ($\lambda = 5.0$). The temperature and concentration profiles in Fig. 2 and 3 show a decreasing trend with the increase of suction parameter (f_w). Thus it reduces the thermal and mass boundary layer thickness with the increase of the suction parameter to a significant amount.

In Fig. 4, we see that the velocity profiles increase with the increase of buoyancy parameter (λ). However near the surface the velocity profiles behaves quite differently for different values of buoyancy parameter (λ). The velocity profiles increase rapidly for $\lambda = 6.0, 10.0$ near the stretching sheet up to $\eta = 0.5$ and then start to decrease. Figure 5 shows the effect of buoyancy parameter (λ) on the temperature field. The

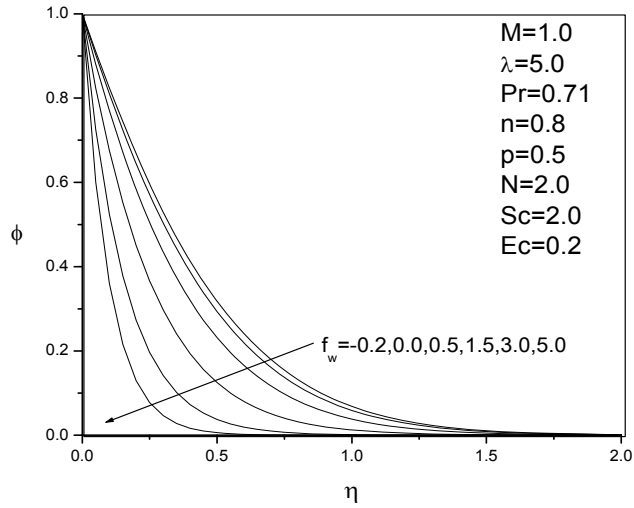


Fig. 3: Concentration profiles for different values of suction parameter (f_w)

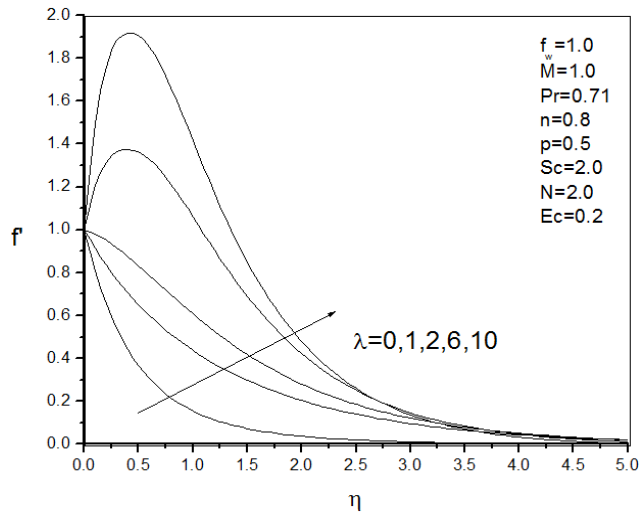


Fig. 4: Effect of buoyancy parameter (λ) on velocity profiles

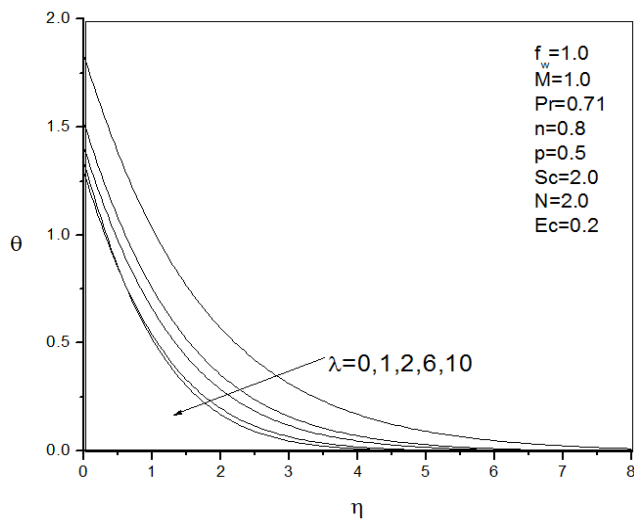


Fig. 5: Effect of buoyancy parameter (λ) on temperature profiles

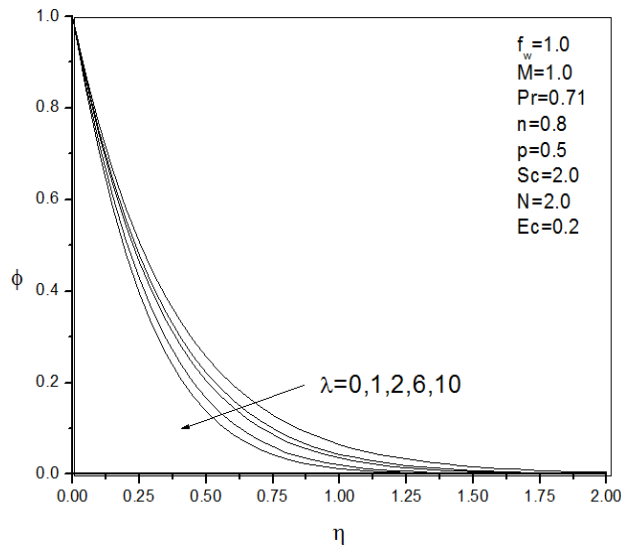


Fig. 6: Effect of buoyancy parameter (λ) on concentration profiles

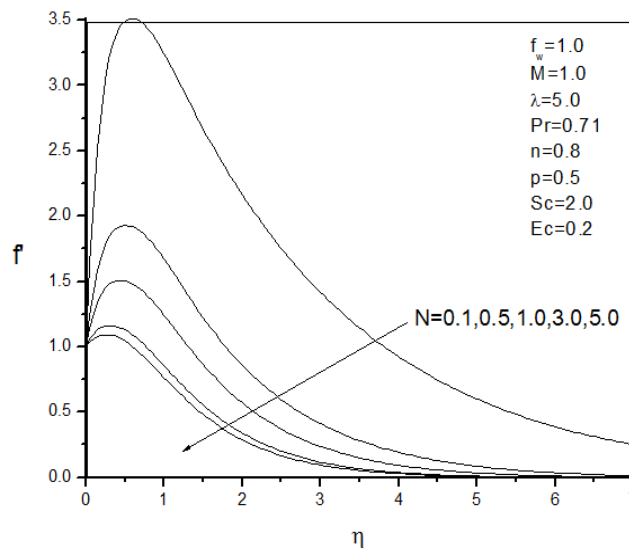


Fig. 7: Velocity profiles for different values of radiation Number (N)

temperature profiles decrease as the buoyancy parameter (λ) increases and for a fixed value of λ , the temperature decreases monotonically. It is observed from Fig. 6 that concentration profiles are strictly decreasing with the increase of buoyancy parameter (λ). It is clear from Fig. 4 to 6 that the buoyancy force has significant effects on the entire flow field. As λ increases the velocity profiles stabilize more quickly and near $\eta = 3.5$, we observed a cross flow in the velocity field (Fig. 4). The case $\lambda = 0$ corresponds to forced convection flow. We thus see that, the velocity profiles stabilize more quickly for forced convection flow.

It is quite clear from both Fig. 7 and 8 that velocity and temperature profiles decrease as the radiation parameter (N) increases. However, the velocity profiles

rise near the stretching sheet for all values of N up to $\eta = 0.6$. It also clears the fact that the velocity profile and wall temperature decreases very rapidly for $N \geq 1.0$ to indicate that the radiation effect can be used to control the velocity and temperature of the boundary layer. The concentration profile in Fig. 9, with increase of radiation parameter (N), the concentration in the vicinity of the boundary layer increases. There is a notable difference in the velocity profiles between the values 0.10 and 0.50 for radiation parameter (N). This is because, at the value of 0.10 the radiation is negligible and upon reaching the value of 0.50, it becomes significant at the velocity field in the velocity boundary layer. With the increase of the radiation parameter (N) the velocity boundary layer thickness reduces rapidly. Due to the radiation from a system, the wall

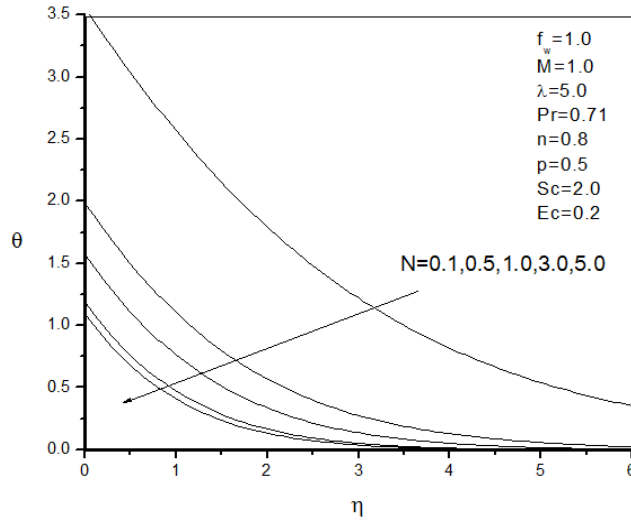


Fig. 8: Temperature profiles for different values of radiation Number (N)

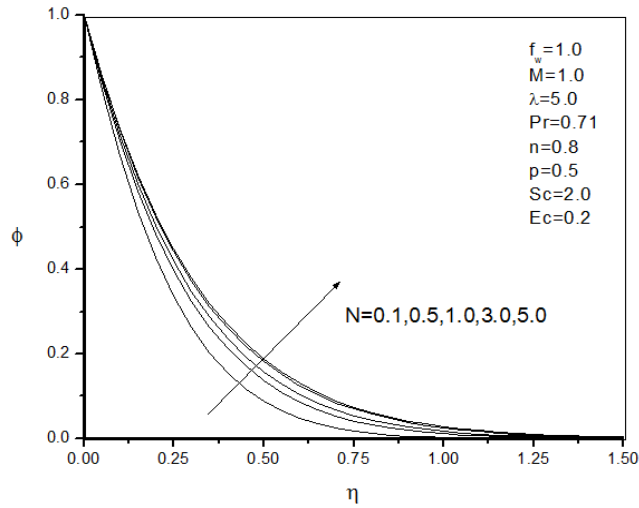


Fig. 9: Concentration profiles for different values of radiation Number (N)

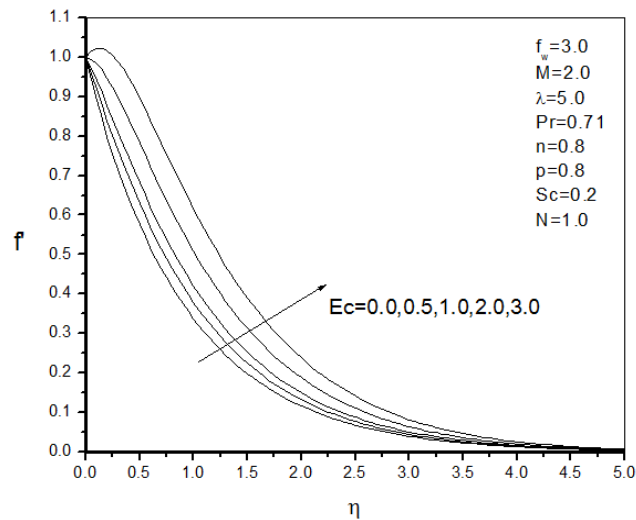


Fig. 10: Effect of Eckert number (Ec) on velocity profiles

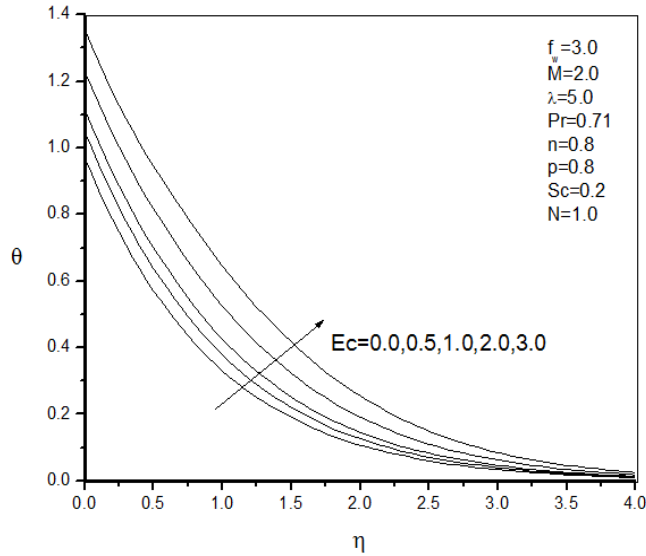


Fig. 11: Effect of Eckert number (Ec) on temperature profiles

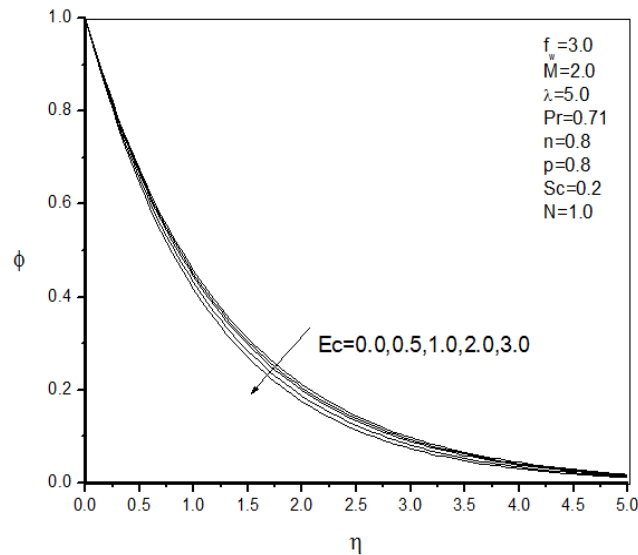


Fig. 12: Effect of Eckert number (Ec) on concentration profiles

temperature decreases to a great extent. From Fig. 8, we find that our numerical results agree with the experimental phenomenon. According to the Newton's law of cooling, the rate of heat transfer is thus increased.

The effects of Eckert number (Ec) on the velocity, temperature and concentration profiles are shown in Fig. 10 to 12, respectively. We observe that the velocity and temperature fields are increasing with the increase of the Eckert number (Ec). The velocity and the temperature profiles show significant change for the increase of Eckert number (Ec). The temperature in the vicinity of the boundary layer increases more rapidly in Fig. 11. There is a notable difference in the temperature profiles between the values $Ec = 2.0$ and 3.0 but very

small difference for the values Ec are $0.0, 0.5, 1.0$. The thermal boundary layer thickness decreases with the increase of the Eckert number (Ec) with the increase of the Eckert number (Ec) the thermal boundary layer thickness reduces rapidly. On the other hand in the Fig. 12, we see that the concentration profiles slightly decrease with the increase of the Eckert number (Ec). It is clear that the Eckert number (Ec) has significant effects on the entire flow field.

The effect of Schmidt number (Sc) on the velocity, temperature and concentration field are shown in Fig. 13 to 15. Physically Schmidt number $Sc = 0.6$ and 1.0 correspond to water vapor and methanol respectively at $25^{\circ}C$ and $1 atm$. So, we observed that the presence of a heavier species (large Schmidt

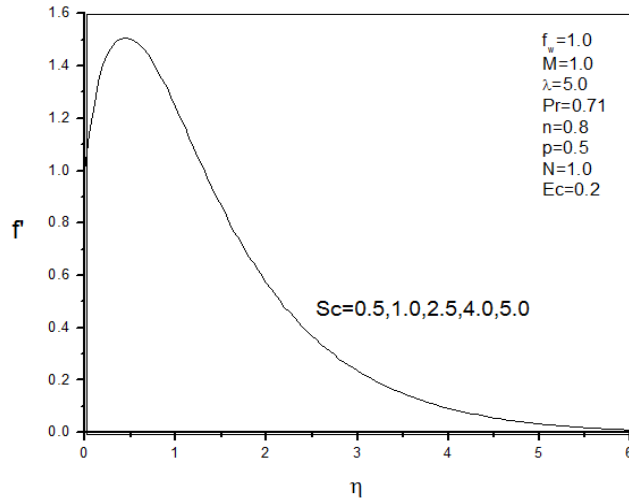


Fig. 13: Schmidt number (Sc) effect on velocity profiles

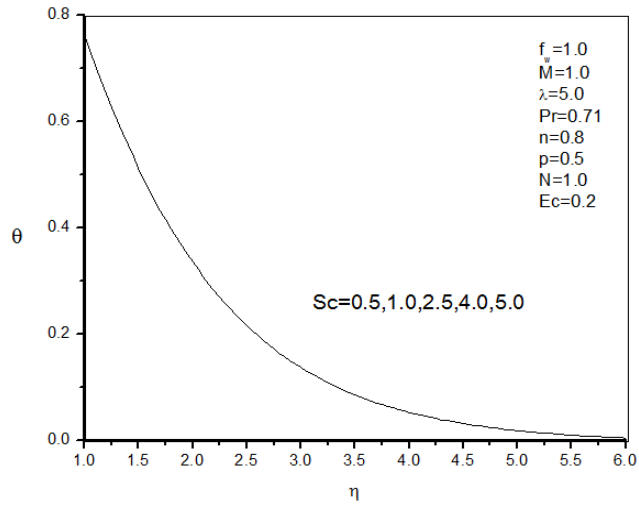


Fig. 14: Schmidt number (Sc) effect on temperature profiles

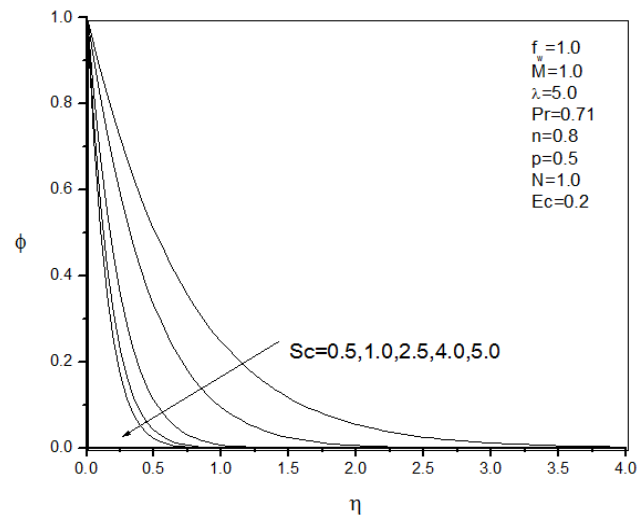


Fig. 15: Schmidt number (Sc) effect on concentration profiles

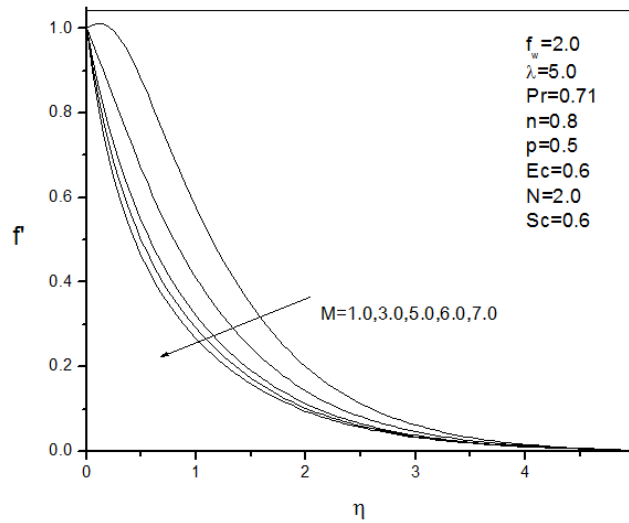


Fig. 16: Velocity profiles for different values of Magnetic field parameter (M)

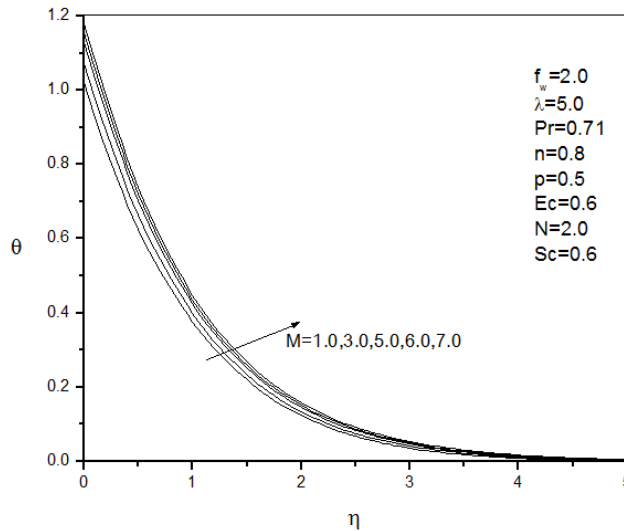


Fig. 17: Temperature profiles for different values of Magnetic field parameter (M)

number) in air ($Pr = 0.71$), the velocity and temperature field remain unchanged as seen from Fig. 13 and 14. On the other hand, Fig. 15 for concentration profiles show a sharp variation with the increase of Schmidt number (Sc).

It is clear from this figure that the concentration profiles decrease to a large extent due to the increase of Schmidt number (Sc). This happens due to the increase of the Schmidt number (Sc), the kinematic viscosity increases and mass diffusion coefficient decreases causing the concentration profiles decrease rapidly.

From Fig. 16 we observe that the magnetic field produces a retarded action on the velocity field and decreases the velocity at a higher rate. As a result momentum boundary layer thickness decreases with the increase of the Magnetic field parameter (M). In Fig. 17 the heat transfer increase with the increase of the magnetic field strength. This implies that the

thermal boundary layer thickness increases a small amount with the increase of the Magnetic field parameter (M). The concentration profiles in Fig. 18 also show a smaller pattern of decreasing transfer rate due to the Magnetic field parameter (M).

Figure 19 and 20 display the effect of Prandtl number (Pr) on velocity and temperature profiles respectively. From both the figure we observe that the velocity and temperature profiles decrease with the increase of Prandtl number (Pr). However, for $Pr = 0.71$, there is a sharp rise in the velocity boundary layers near the stretching sheet. Physically $Pr = 0.71$ corresponds to air at 20°C . From Fig. 20 we see that for small Pr wall temperature is very high compared to larger values. It is clear from this figure that, for large values of Prandtl number the wall temperature is very small and so the rate of heat transfer increases rapidly for the high viscous fluids, such as

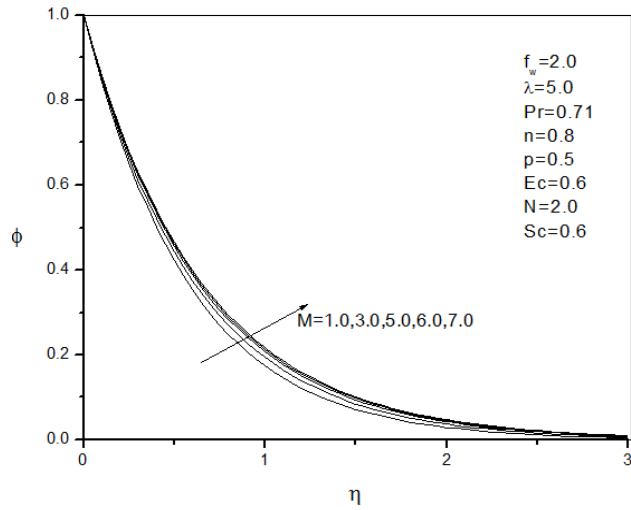


Fig. 18: Concentration profiles for different values of Magnetic field parameter (M)

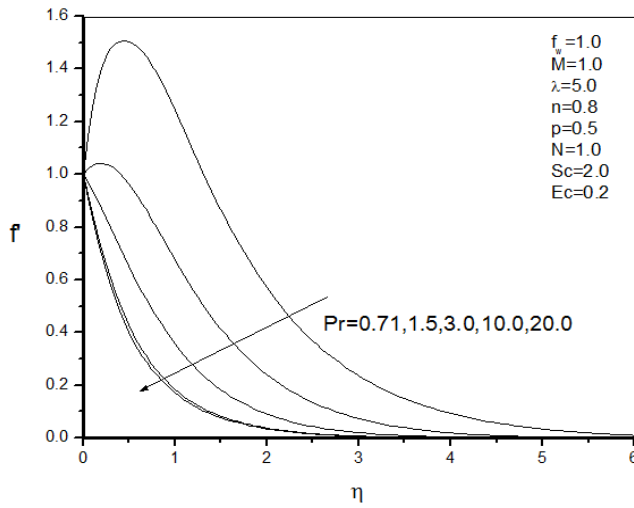


Fig. 19: Velocity profiles for different values of Prandtl number (Pr)

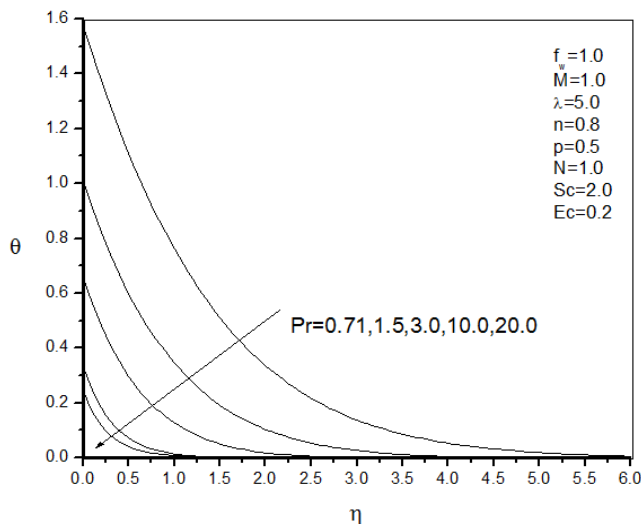


Fig. 20: Temperature profiles for different values of Prandtl number (Pr)

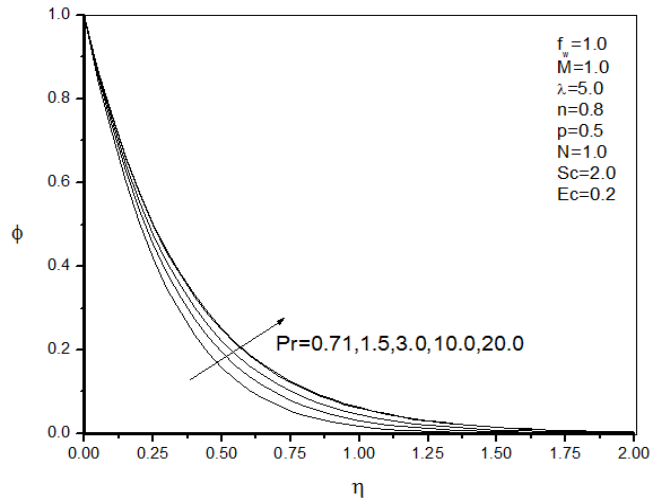


Fig. 21: Concentration profiles for different values of Prandtl number (Pr)

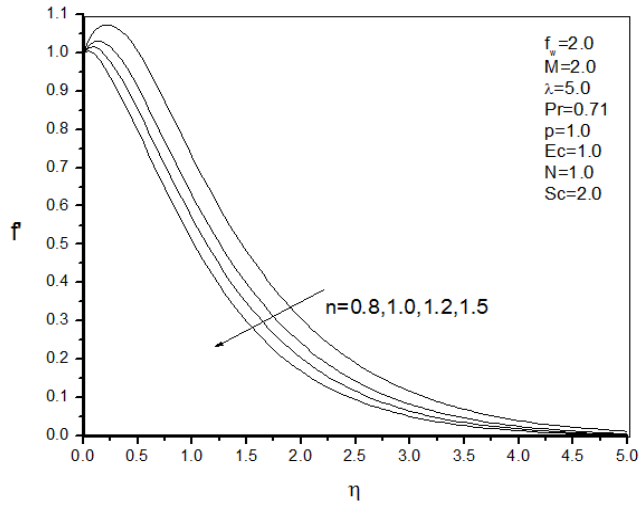


Fig. 22: Velocity profiles for different values of power-law fluid index (n)

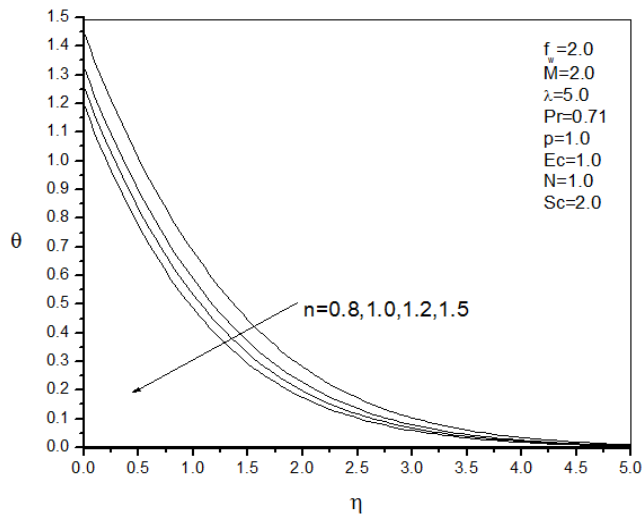


Fig. 23: Temperature profiles for different values of power-law fluid index (n)

petroleum oils and lubricants (typical values of Prandtl number are 10,000 to 40,000 at 20°C) Conveniently if for large values of Pr ($Pr \gg 1$), then momentum boundary layer is thicker than thermal boundary layer. The opposite behavior is visible for smaller values of Pr ($Pr \ll 1$), so that the drag of the wall decreased. From above investigations, it follows that Pr strongly influences the relative growth of the velocity and thermal boundary layers. On the other hand, in Fig. 21 the concentration profiles increase with the increase of Prandtl number (Pr).

Figure 22 illustrates that the velocity profile decreases with the increase of power-law fluid index (n) for flows where the surface is accelerated. The temperature profiles also decrease with the increase of power-law fluid index (n) for $p = 1$ in the Fig. 23. We see that the effect of power-law fluid index (n) is more

noticeable for accelerated surface flows. Concentration profiles (Fig. 24) have a little change with the increase of the power-law fluid index (n) for flows where the surface is accelerated.

The effect of velocity index (p) on velocity, temperature and concentration profiles are shown in the Fig. 25 to 27 for pseudo-plastic. It is clear from Fig. 25 and 27 that, velocity and concentration profiles decrease with increasing velocity index (p) for pseudo-plastic fluids and in the Fig. 26 temperature profiles are slightly increase with the increase of the velocity-index (p) and there is a cross flow near $\eta = 2.0$, in the temperature profiles.

Table 1 shows the comparison of the skin friction coefficient and the local heat transfer for various values of n and M with $p = 0.5$ and $Pr = 5.0$. We see that the results agree well among these two sets.

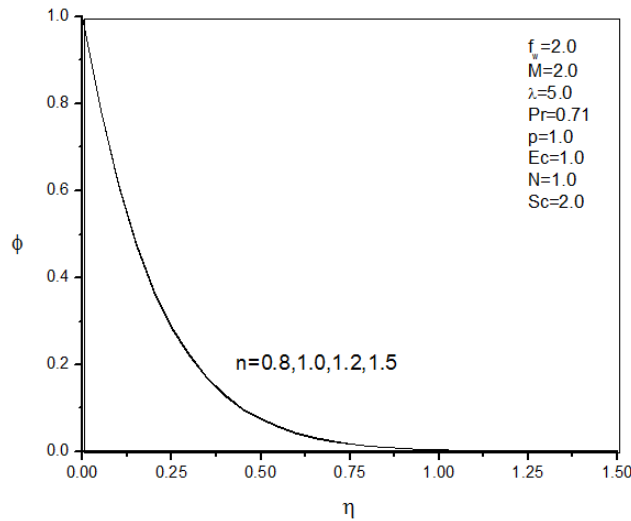


Fig. 24: Concentration profiles for different values of power-law fluid index (n)

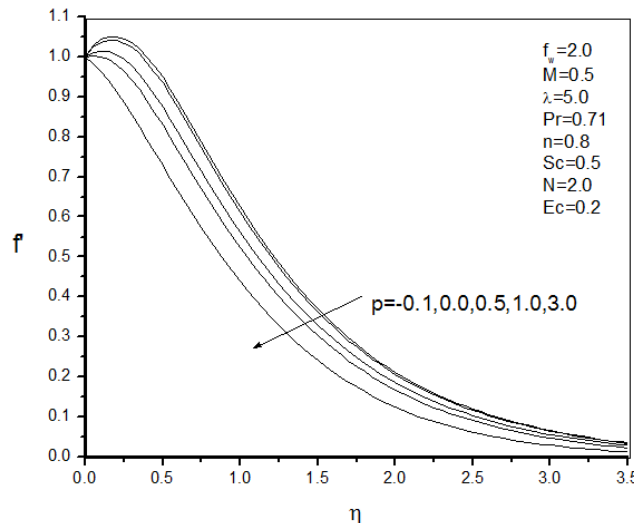


Fig. 25: Effect of velocity index (p) on velocity profiles for pseudo-plastic fluid

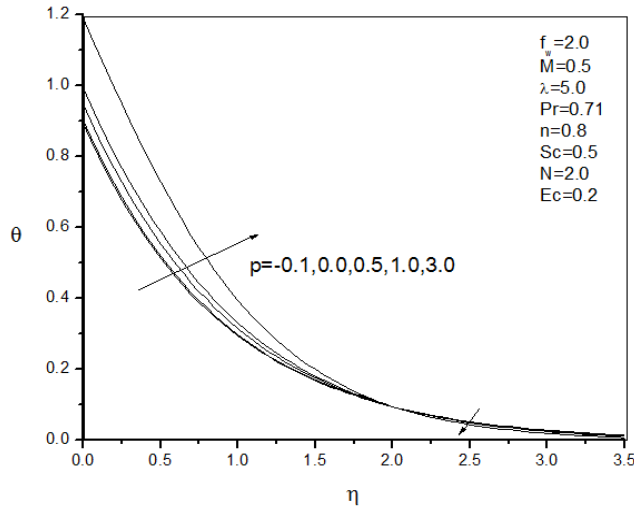


Fig. 26: Effect of velocity index (p) on temperature profiles for pseudo-plastic fluid

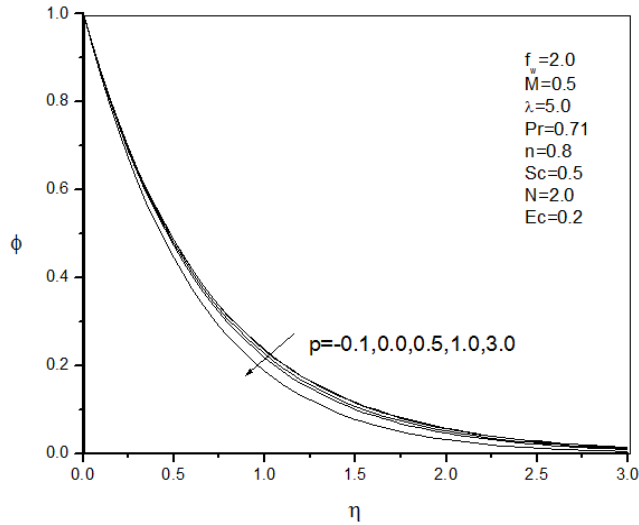


Fig. 27: Effect of velocity index (p) on concentration profiles for pseudo-plastic fluid

Table 1: Comparison of $Re_x^{1/(n+1)} C_f$ and $Nu_x Re_x^{-1/(n+1)}$ with Chen (2008)

Parameters			$Re_x^{1/(n+1)} C_f$		$Nu_x Re_x^{-1/(n+1)}$	
n	M	f_w	Chen (2008)	Present study	Chen (2008)	Present study
0.5	1	-0.2	-2.472213	-2.4723340	0.791413	0.7913201
		0.0	-2.633241	-2.6334386	1.346116	1.3461035
		0.6	-3.213067	-3.2137484	3.683003	3.6833107
	5	-0.2	-3.881351	-3.8813143	0.367234	0.3679528
		0.6	-4.608094	-4.6078741	3.528467	3.5287845
		-0.2	-2.323803	-2.3238161	1.019734	1.0198238
1.0	1	0.0	-2.519363	-2.5193782	1.578424	1.5785883
		0.6	-3.198565	-3.1985827	3.866662	3.8672224
		-0.2	-4.529439	-4.5294577	0.692476	0.6935165
	5	0.0	-4.726210	-4.7262298	1.320497	1.3231287
		0.6	-5.366930	-5.3668243	3.754876	3.7553935
		-0.2	-2.189081	-2.1891280	1.127959	1.1284628
1.5	1	0.0	-2.412287	-2.4121919	1.689593	1.6902300
		0.6	-3.178401	-3.1782320	3.958697	3.9593387
		0.6	-5.768535	-5.7687145	3.874307	3.8749347
	5	0.0	-1.073300	-1.0734818	1.278189	1.2783778
		-0.2	-2.107985	-2.1080359	1.180071	1.1812444
		0.6	-5.977131	-5.9770460	3.935870	3.9357910

Table 2: Effect of n , M and f_w on C_f , Nu_x and Sh

Parameters			Free convection with radiation $\lambda = 5.0, N = 1.0$		
n	M	f_w	C_f	Nu_x	Sh
0.6	1.0	1.0	5.264750	0.536082	3.29987
		1.5	3.974640	0.635992	3.97954
		3.0	-1.186730	0.997035	6.48335
	3.0	2.0	-0.039990	0.725500	4.68486
		2.5	-1.612990	0.850684	5.54325
		2.0	-1.676720	0.709880	4.63363
0.8	1.0	3.0	-4.281140	0.972863	6.39494
		1.0	3.816830	0.650228	3.26945
		2.0	1.325700	0.837286	4.79536
	3.0	2.5	0.097624	0.944556	5.64231
		-1.0	6.115540	0.342521	1.19179
		1.0	1.913010	0.610548	3.17996
1.0	3.0	2.0	-0.630960	0.805520	4.73165
		-1.0	5.132230	0.314287	1.13649
		0.5	1.697280	0.497702	2.44933
	1.0	2.0	-2.106910	0.782430	4.68398
		-1.0	6.958430	0.415016	1.22469
		0.5	4.396140	0.605018	2.62146
1.2	3.0	2.0	1.082240	0.863684	4.81610
		2.0	-0.753100	0.829360	4.74915
		3.0	-3.468040	1.059710	6.51213
	5.0	1.5	-0.961169	0.701110	3.87880
		2.0	-2.231640	0.805380	4.70437
		3.0	-4.842540	1.044780	6.48849
1.5	1.0	0.5	3.901270	0.643044	2.63389
		2.0	0.894858	0.893405	4.84117
		2.0	-0.875741	0.856035	4.77040
	3.0	1.5	-1.100280	0.729150	3.90034

Table 2 lists the present calculations for the flow and heat and mass transfer characteristics, including the skin friction coefficient ($Re_x^{1/(n+1)}C_f$), the Nusselt number ($Nu_x Re_x^{-1/(n+1)}$) and the Sherwood number ($Sh Re_x^{-1/(n+1)}$) for various values of n, M and f_w with $Pr = 0.71, p = 1.0, Ec = 0.2$ and $Sc = 0.2$.

CONCLUSION

The problem has dealt with the two dimensional heat and mass transfer free convection flow of an MHD Non-Newtonian power-law fluid along stretching sheet in the presence of magnetic field with thermal radiation and viscous dissipation. From the present investigation we can make the following conclusions:

- For the increase of the suction parameter (f_w), the velocity, temperature and concentration profiles decrease significantly. So, suction stabilizes the velocity, temperature and concentration field quickly to prevent the boundary layer separation.
- Larger values of buoyancy parameter (λ) can be used to control the temperature and concentration fields.
- The temperature and concentration fields are highly influenced by Prandtl number (Pr).
- The momentum boundary layer and the thermal boundary layer thickness reduce as a result of increasing radiation.

- The presence of a heavier species (large Sc) in the flow field decrease the rate of concentration in the boundary layer.
- The velocity and temperature profiles increase while the concentration profiles decrease with the increase of the Eckert number (Ec). This parameter plays important rule in case of non-Newtonian fluids compared to Newtonian fluids. The effects of Eckert number (Ec) on velocity, temperature and concentration fields are significant.
- Using magnetic field we can control the flow characteristics as it has significant effects on heat and mass transfer.
- Drag of the pseudo-plastics along a stretched surface decreases as the velocity index increases.

REFERENCES

Ali, M.M., T.S. Chen and B.F. Armaly, 1984. Natural convection interaction in boundary-layer flow over horizontal surfaces. *AIAA J.*, 22: 1797-1803.

Anderson, H.I., K.H. Bech and B.S. Dandapat, 1992. Magneto hydrodynamic flow of a power-law fluid over a stretching sheet. *Int. J. Nonlin. Mech.*, 27: 926-936.

Chamkha, A.J., H.S. Takhar and V.M. Soundalgekar, 2001. Radiation effects on free convection flow past a semi-infinite vertical plate with mass transfer. *Chem. Eng. J.*, 84: 335-342.

- Chen, C.H., 2008. Effects of magnetic field and suction/injection on convective heat transfer on non-Newtonian power-law fluids past a power-law stretched sheet with surface heat flux. *Int. J. Therm. Sci.*, 47: 954-961.
- Chen, H.T. and C.K. Chen, 1988. Free convection of non-Newtonian fluids along a vertical plate embedded in a porous medium. *Trans. ASME, J. Heat Transfer*, 110: 257-260.
- Dandapat, B.S. and A.S. Gupta, 2005. Flow and heat transfer in a viscoelastic fluid over a stretching sheet. *Int. J. Nonlin. Mech.*, 40: 215-219.
- Datti, P.S., K.V. Prasad, M.S. Abel and A. Joshi, 2005. MHD viscoelastic fluid flow over a non-isothermal stretching sheet. *Int. J. Eng. Sci.*, 42: 935-946.
- Elbashbeshy, E.M.A., 1998. Heat transfer over a stretching surface with variable surface heat flux. *J. Phys. D Appl. Phys.*, 31:1951-1954.
- El-Hakim, M.A., 2008. Radiative effects on non-darcy natural convection from a heated vertical plate in saturated porous media with mass transfer for non-Newtonian fluid. *J. Porous Media*, 12: 89-99.
- Glauert, M.B., 1961. A study of the magnetohydrodynamic boundary layer on a flat plate. *J. Fluid Mech.*, 10: 276-288.
- Mahmod, M.A.A. and M.A.E. Mahmoud, 2006. Analytical solutions of hydro magnetic boundary layer flow of non-Newtonian power-law fluid past a continuously moving surface. *Acta Mech.*, 181: 83-89.
- Nachtsheim, P.R. and P. Swigert, 1965. Satisfaction of the asymptotic boundary conditions in numerical solution of the systems of non-linear equations of boundary layer type. Ph.D. Thesis, NASA TN D-3004, Washington DC.
- Rahaman, M.M. and M.A. Sattar, 2006. Magnetohydrodynamic convective flow of a micropolar fluid past a continuously moving vertical porous plate in the presence of heat generation/absorption. *J. Heat Trans-T. ASME*, 128: 142-152.
- Rajgopal, K.R., T.Y. Na and A.S. Gupta, 1984. Flow of a viscoelastic fluid over a stretching sheet. *Rheol. Acta*, 23: 213-215.
- Raptis, A., 1998. Flow of a micropolar fluid past a continuously moving plate by the presence of radiation. *Int. J. Heat Mass Tran.*, 41: 2865-2866.
- Sakiadis, B.C., 1961. Boundary-layer behavior on continuous solid surfaces: I. Boundary-layer equations for two-dimensional and axisymmetric flow. *AIChE J.*, 7: 26-28.
- Takhar, H.S., R.S.R. Gorla and V.M. Soundalgekar, 1996. Radiation effects on MHD free convection flow of a radiating fluid past a semi-infinite vertical plate. *Int. J. Numer. Method. H.*, 6: 77-83.
- Vajravelu, K. and A. Hadjinicolaou, 1997. Convective heat transfer in an electrically conducting fluid at a stretching surface with uniform free stream. *Int. J. Eng. Sci.*, 35(12-13): 1237-1244.